J. Fluid Mech. (1976), *vol.* 74, *part* 4, *pp.* 593–610
Printed in Great Britain

Contribution towards a Reynolds-stress closure for low-Reynolds-number turbulence

By K. HANJALIĆ† AND B. E. LAUNDER
Department of Mechanical Engineering, Imperial College, London

(Received 12 February 1975)

The problem of closing the Reynolds-stress and dissipation-rate equations at low Reynolds numbers is considered, specific forms being suggested for the direct effects of viscosity on the various transport processes. By noting that the correlation coefficient $\overline{uv^2}/\overline{u^2}\,\overline{v^2}$ is nearly constant over a considerable portion of the low-Reynolds-number region adjacent to a wall the closure is simplified to one requiring the solution of approximated transport equations for only the turbulent shear stress, the turbulent kinetic energy and the energy dissipation rate. Numerical solutions are presented for turbulent channel flow and sink flows at low Reynolds number as well as a case of a severely accelerated boundary layer in which the turbulent shear stress becomes negligible compared with the viscous stresses. Agreement with experiment is generally encouraging.

1. Introduction

There is currently much activity in developing and refining so-called 'second-order' closures for turbulent flow. In these schemes the Reynolds stresses $\overline{u_i u_j}$ are obtained from an approximated set of transport equations containing only mean-field variables and second-order turbulence correlations, i.e. correlations of just two fluctuating quantities. The aim of this research area is to devise (in terms of the allowable correlations) sufficiently faithful imitations of the *real* processes affecting the transport of $\overline{u_i u_j}$ for the equations to provide a generally valid closure for determining the Reynolds stress. (Here 'valid' means offering sufficient accuracy for practical purposes.)

Whether this aim can be completely achieved remains an open question. Systematic and extensive testing has so far been confined to thin shear flow (because the numerical task of solving the equations for more complicated flows is still not a light one). For these flows, at least, two of the recently proposed schemes, those of Lumley & Khajeh Nouri (1973) and Launder, Reece & Rodi (1975), do give reasonably correct predictions of $\overline{u_i u_j}$ for a range of flows. Both treatments, however, neglected any direct effect of viscosity on the turbulence structure. While viscous effects on the energy-containing turbulence motions are indeed negligible throughout most of the flow, the condition of no slip at solid interfaces always ensures that in the immediate vicinity of a wall viscous effects will be influential, perhaps dominant.

Although the thickness of this viscosity-affected zone is usually two or more

† Present address: Mašinski Fakultet, Sarajevo 71,000, Jugoslavia.

orders of magnitude less than the overall width of the flow, its effects extend over the whole flow field since, typically, 50 % of the velocity change from the wall to the free stream occurs in this region. Now, it is possible to avoid the complications of the viscosity-affected region by drawing on the fact that, in many turbulent flows, the important mean and turbulent flow quantities are functions only of the normal distance from the wall (provided all variables are non-dimensionalized by the wall shear stress, the density and the fluid viscosity). Thus, in making calculations of flow over rigid surfaces all the dependent variables appearing in the closure scheme are matched to the 'universal' values at some point beyond the viscosity-dependent region. This approach has been followed in the work of Bradshaw, Ferriss & Atwell (1967), Hanjalić & Launder (1972) and Launder *et al.* (1975) as well as in numerous simpler closures where the Reynolds stresses are uniquely related to the mean velocity field.

The near-wall region is insufficiently universal, however, for the above approach to be satisfactory in all circumstances. Transpiration through the wall, steep streamwise pressure gradients, swirl (as, for example, near a spinning disk), and steep temperature gradients (due to large imposed wall heat fluxes or to frictional heating) are just a few of the influences that may cause this region to differ from its so-called 'universal' behaviour. To account for these various influences it is necessary to extend the calculations up to the wall itself.

This approach is commonplace when the mixing-length hypothesis or some other very rudimentary turbulence model is used. The ratio of mixing length to normal distance from the wall is held to be a function of a normal-distance Reynolds number $x_2 U^*/\nu$, where the velocity scale U^* is taken (according to taste) as either the local or the wall friction velocity (or sometimes a combination of the two). The functional relation is easily correlated by reference, say, to profiles of mean velocity in pipe flow, cf. Van Driest (1956). There have been similar approaches to extending Prandtl's (1945) model (in which a transport equation is solved for the turbulence kinetic energy k) to the low-Reynolds-number regime. Here the work of Glushko (1965), Beckwith & Bushnell (1968) and Wolfshtein (1969) may be mentioned. Although models of this kind display adequately correct behaviour when the stress is essentially uniform near the wall, they achieve little improvement over the assumption of a universally similar near-wall region unless additional empirical modifications are made to the mixing length to account for effects of transpiration, pressure gradient, etc.

Of course, a principal reason for devising a second-order closure for low-Reynolds-number turbulence is to provide a more reliable basis for calculating wall-bounded flows than is offered by the use of either 'wall-law' matching or the mixing-length hypothesis. The present contribution reports our progress in this direction. The work has sought to extend the closure for high Reynolds numbers reported by Launder *et al.* (1975). However, to limit the sheer task of obtaining numerical solutions, we have simplified the model so that, for two-dimensional shear layers, the turbulent shear stress and the turbulence kinetic energy are the only Reynolds-stress elements calculated. The dissipation rate ϵ of turbulence energy (which appears as an unknown in both the kinetic energy and shear-stress equations) is found from a transport equation similar to (though with important

differences from) that devised and tested by Jones & Launder (1972*a*, 1973). Applications are reported for grid turbulence in the final period of decay as well as for low-Reynolds-number channel flow and strongly accelerated boundary layers.

2. Proposals for closure at low Reynolds numbers

2.1. *The stress transport equations*

For an incompressible turbulent flow the exact equation governing the transport of Reynolds stress $\overline{u_i u_j}$ (see, for example, Hinze 1959, p. 250) may be written as

$$\frac{D\overline{u_i u_j}}{Dt} = -\underbrace{\left\{\overline{u_j u_k}\frac{\partial U_i}{\partial x_k} + \overline{u_i u_k}\frac{\partial U_j}{\partial x_k}\right\}}_{\text{(i)}} + \underbrace{\overline{\frac{p}{\rho}\left(\frac{\partial u_i}{\partial x_j} + \frac{\partial u_j}{\partial x_i}\right)}}_{\text{(ii)}}$$

$$+ \underbrace{\frac{\partial}{\partial x_k}\left\{\nu\frac{\partial \overline{u_i u_j}}{\partial x_k} - \overline{u_i u_j u_k} - \overline{\frac{p}{\rho}(\delta_{jk}u_i + \delta_{ik}u_j)}\right\}}_{\text{(iii)}} \underbrace{- 2\nu\overline{\frac{\partial u_i}{\partial x_k}\frac{\partial u_j}{\partial x_k}}}_{\text{(iv)}}, \tag{2.1}$$

where the notation is the same as in Launder *et al.* (1975). That paper (LRR) made proposals for closing (2.1) which led to satisfactory predictions of $\overline{u_i u_j}$ (and of the mean flow field) in a number of thin shear flows at high Reynolds numbers. Here we adopt the same closure approximations as in LRR, extending them (and introducing additional ones where necessary) to account for low-Reynolds-number effects.

The stress-generation terms may be treated exactly with a second-order closure; approximations are needed for terms (ii)–(iv). The pressure fluctuations that appear in term (ii) satisfy the equation

$$\frac{1}{\rho}\frac{\partial^2 p}{\partial x_i^2} = -\left(\frac{\partial^2(u_i u_j - \overline{u_i u_j})}{\partial x_i \partial x_j} + 2\frac{\partial u_i}{\partial x_j}\frac{\partial U_j}{\partial x_i}\right), \tag{2.2}$$

obtained by taking the divergence of the equation of motion. Since the fluid viscosity makes no explicit appearance in (2.2) it is assumed that, to first order, the high-Reynolds-number form of the pressure–strain correlation adopted in LRR may be retained, i.e.

$$\overline{\frac{p}{\rho}\left(\frac{\partial u_j}{\partial x_i} + \frac{\partial u_i}{\partial x_j}\right)} = -c_1\frac{\epsilon}{k}(\overline{u_i u_j} - \tfrac{2}{3}\delta_{ij}k) - \frac{(c_2+8)}{11}\{P_{ij} - \tfrac{2}{3}\delta_{ij}k\}$$

$$- \frac{(30c_2-2)}{55}k\left\{\frac{\partial U_i}{\partial x_j} + \frac{\partial U_j}{\partial x_i}\right\} - \frac{(8c_2-2)}{11}\{D_{ij} - \tfrac{2}{3}P\delta_{ij}\} + \phi_{ij,w}, \tag{2.3}$$

where k and ϵ are the turbulent kinetic energy and the correlation $\nu\overline{(\partial u_i/\partial x_k)^2}$ respectively, P is the rate of generation of turbulence energy by mean-strain effects, and

$$P_{ij} \equiv -\left\{\overline{u_i u_k}\frac{\partial U_j}{\partial x_k} + \overline{u_j u_k}\frac{\partial U_i}{\partial x_k}\right\}, \quad D_{ij} \equiv -\left\{\overline{u_i u_k}\frac{\partial U_k}{\partial x_j} + \overline{u_j u_k}\frac{\partial U_k}{\partial x_i}\right\}.$$

Following LRR the coefficients c_1 and c_2 take the constant values 1·5 and 0·4. The term $\phi_{ij,w}$ stands for a wall-proximity effect on the pressure–strain

correlation, details of which appear in LRR. Close to a wall this term causes about 30 % of the total turbulence energy to be transferred from the stress component normal to the wall, $\overline{u_2^2}$, to that in the direction of the mean flow, $\overline{u_1^2}$. The direct effect on the shear stress $\overline{u_1 u_2}$ is however rather small (there is an indirect effect due to the appearance of $\overline{u_1^2}$ and $\overline{u_2^2}$ in the shear-stress equation); thus, since it is the shear stress which controls the mean velocity field, we neglect the term $\phi_{ij,w}$ entirely here. In § 3.2 we suggest a very simple way of accounting for the wall effects on the normal stresses.

Turning to the diffusive transport terms in (2.1), the molecular transport of stress $\nu\,\overline{\partial u_i u_j}/\partial x_j$, which is negligible at high Reynolds numbers, of course needs no further approximation. There seems no reason to suppose that viscous effects on the other diffusion terms should be small; indeed an examination of the transport equation for $\overline{u_i u_j u_k}$ suggests the contrary. However, it seems safe to assume that for values of x_2^+ down to about 15 the contribution of diffusive transport to the stress budget is barely significant, the main factors being the local stress generation and dissipation rates and the contribution of the pressure–strain term. Moreover, for values of x_2^+ below about 8 molecular diffusion will progressively outweigh turbulent diffusion. It is clear, therefore, that a poor approximation of the turbulent transport terms will affect the stress profiles over only a small proportion of the viscous-affected region. We therefore retain the approximation proposed originally by Hanjalić & Launder (1972) and used in LRR:

$$-\overline{u_i u_j u_k} = c_s \frac{k}{\epsilon}\left\{\overline{u_k u_l}\frac{\partial \overline{u_i u_j}}{\partial x_l} + \overline{u_j u_l}\frac{\partial \overline{u_k u_i}}{\partial x_l} + \overline{u_i u_l}\frac{\partial u_j u_k}{\partial x_l}\right\}. \tag{2.4}$$

Pressure transport was neglected by LRR. Though there is no certainty that these terms are negligible in the strongly inhomogeneous near-wall region, we again call on the principle of limited effectiveness used to support the use of (2.4); accordingly we take no account of this process.

The one term in (2.1) where it *is* essential to include viscous effects is term (iv), the dissipative correlation. At sufficiently high Reynolds numbers the fine-scale motion will be essentially isotropic and hence

$$2\nu\overline{\frac{\partial u_i}{\partial x_k}\frac{\partial u_j}{\partial x_k}} = \tfrac{2}{3}\delta_{ij}\epsilon. \tag{2.5}$$

As the Reynolds number approaches zero the energy-containing and dissipation range of motions overlap and the dissipation rate is then commonly approximated (for example, Rotta 1951) as

$$\nu\overline{\frac{\partial u_i}{\partial x_k}\frac{\partial u_j}{\partial x_k}} = \frac{\overline{u_i u_j}}{k}\epsilon. \tag{2.6}$$

These two asymptotic forms† have led a number of workers to propose that in general the correlation may be approximated as

$$\nu\overline{\frac{\partial u_i}{\partial x_k}\frac{\partial u_j}{\partial x_k}} = \tfrac{2}{3}\epsilon\left\{(1-f_s)\,\delta_{ij} + \frac{\overline{u_i u_j}}{\frac{2}{3}k}f_s\right\}, \tag{2.7}$$

† Two referees have drawn attention to the fact that (2.6) does not have the status of an asymptotically *valid* relation, however.

where f_s is a function of the turbulent Reynolds number $R_T = k^2/\nu\epsilon$; its value changes from unity to zero as the Reynolds number varies from zero to infinity. It would appear that, even if (2.7) is adequate, the function f_s ought to depend also on the amount of mean strain felt by a typical dissipative eddy during its lifetime. For the straining will impart a directional orientation on the fine-scale structure which, in crude terms, will make the dissipation proceed more according to (2.6) than (2.5). Now, the lifetime of a dissipative motion is of the order of $\nu^{\frac{1}{2}}\epsilon^{-\frac{1}{2}}$ and the time taken for the mean flow to distort such an eddy appreciably is $(\partial U_1/\partial x_2)^{-1}$. Thus the dimensionless parameter expressing the influence of mean strain on f_s is $(\nu/\epsilon)^{\frac{1}{2}}\,\partial U_1/\partial x_2$ or, on regrouping, $R_T^{-\frac{1}{2}}(k\,\partial U_1/\partial x_2)\,\epsilon^{-1}$.

The prospect of correlating a suitable form for f_s in terms of both R_T and $R_T^{-\frac{1}{2}}\,k(\partial U_1/\partial x_2)\,\epsilon^{-1}$ is a rather daunting one however. We have therefore taken no specific account of mean strain on f_s. The perceived effect of $(k\,\partial U_1/\partial x_2)\,\epsilon^{-1}$ will arguably be much weaker than that of R_T:† for an equilibrium flow the former varies by only 20 % or so about the value 3·5 in the range $10 < x_2^+ < 50$ whereas there will be about a fivefold variation of R_T. The best form for f_s that has emerged from the numerical computations presented in § 4 is

$$f_s = (1 + \tfrac{1}{10}R_T)^{-1}, \tag{2.8}$$

which, it will be noted, takes the requisite limiting values for very high and very low R_T.

2.2. *The equation for ϵ transport*

Following Daly & Harlow (1970), an exact equation for the transport of ϵ in a fluid of uniform viscosity is obtained by differentiating the equation of motion for u_i with respect to x_l and multiplying through by $2\nu\,\partial u_i/\partial x_l$. The result may be written as

$$\begin{aligned}\frac{D\epsilon}{Dt} = &\underbrace{-2\nu\overline{\frac{\partial u_i}{\partial x_k}\frac{\partial u_i}{\partial x_l}\frac{\partial u_k}{\partial x_l}}}_{\text{(i)}} \underbrace{-2\overline{\left(\nu\frac{\partial^2 u_i}{\partial x_k\,\partial x_l}\right)^2}}_{\text{(ii)}} \underbrace{-\frac{\partial}{\partial x_k}\left\{\overline{u_k\epsilon'} + \frac{2\nu}{\rho}\overline{\frac{\partial u_k}{\partial x_l}\frac{\partial p}{\partial x}} - \nu\frac{\partial \epsilon}{\partial x_k}\right\}}_{\text{(iii)}} \\ &\underbrace{-2\nu\left\{\overline{\frac{\partial u_i}{\partial x_l}\frac{\partial u_k}{\partial x_l}} + \overline{\frac{\partial u_l}{\partial x_i}\frac{\partial u_l}{\partial x_k}}\right\}\frac{\partial U_i}{\partial x_k}}_{\text{(iv)}} \underbrace{-2\nu\,\overline{u_k\frac{\partial u_i}{\partial x_l}}\frac{\partial^2 U_i}{\partial x_k\,\partial x_l}}_{\text{(v)}}.\end{aligned} \tag{2.9}$$

Tennekes & Lumley (1972, p. 90) have inferred from an order-of-magnitude analysis of (2.9)‡ that, at high turbulent Reynolds numbers, terms (i) and (ii) (representing generation of ϵ by stretching of vortex filaments and destruction through the tendency of viscosity to reduce instantaneous velocity gradients) far outweigh all other terms; their *difference*, however (which is what matters), is ordinarily of the same magnitude as the diffusive transport terms (iii). Terms (iv) and (v) are smaller than the other terms by a factor proportional to $R_T^{\frac{1}{2}}$ and R_T respectively; at high Reynolds numbers, therefore, these may be omitted, together with the viscous diffusion term in (iii).

† Provided that attention is limited to cases where the low-Reynolds-number region is adjacent to a wall.

‡ Or, rather, of the closely related equation for the square of the vorticity fluctuations.

The following analogue form of (2.9) has been used to calculate a number of high-Reynolds-number flows (see Reynolds 1970; Hanjalić & Launder 1972; LRR):

$$\frac{D\epsilon}{Dt} = c_{\epsilon 1}\frac{\epsilon}{k}P - c_{\epsilon 2}\frac{\epsilon^2}{k} - c_\epsilon \frac{\partial}{\partial x_k}\left\{\frac{k}{\epsilon}\overline{u_k u_l}\frac{\partial \epsilon}{\partial x_l}\right\}. \tag{2.10}$$

The first two terms on the right of (2.10) approximate the difference between terms (i) and (ii) of (2.9)† while the third represents diffusive transport. Lumley (1972) omitted the first term in (2.10) on the grounds that the terms in (2.9) containing mean-field variables were all of lower order. The analogue equation clearly needs to contain some positive source term however; otherwise one could arrange to increase indefinitely the level of turbulence energy by straining the turbulence field while the dissipation rate decreased monotonically. Lumley & Khajeh Nouri (1973) have argued that the quantity $(\overline{u_i u_j}/k - \frac{2}{3}\delta_{ij})^2\epsilon$ should appear in place of P. It does seem more reasonable that the small imbalance between (i) and (ii) in (2.9) should be affected by the skewness of the energy-containing motions rather than by the mean field directly. However, it is the presence of mean strain which causes the anisotropy and, except where transport effects on turbulence are large, $(\overline{u_i u_j}/k - \frac{2}{3}\delta_{ij})^2$ and P/ϵ vary in much the same way throughout a turbulent flow. Thus, since (2.10) has been extensively tested in numerical computations it has been adopted as the high-Reynolds-number asymptote in the present work.

In a homogeneous decaying turbulent flow (2.10) becomes simply

$$D\epsilon/Dt = -c_{\epsilon 2}\epsilon^2/k. \tag{2.11a}$$

It is easily shown that (2.11) causes the kinetic energy to decay at a rate proportional to x^{-n}, where $n = (c_{\epsilon 2} - 1)^{-1}$. At high Reynolds numbers the extensive grid-turbulence data of Comte-Bellot & Corrsin (1966) indicate the exponent n to be about 1·2, suggesting that $c_{\epsilon 2}$ should be approximately 1·8. Far behind the grid the decay pattern undergoes a rather abrupt change: the exponent n increases to an asymptotic value of 2·5. We assume that this variation is due entirely to the diminution of R_T and hence write, in general,

$$D\epsilon/Dt = -c_{\epsilon 2}f_\epsilon \epsilon^2/k, \tag{2.11b}$$

where f_ϵ is a function of R_T, taking the value unity at high Reynolds number. The form of dependence is chosen by reference to Batchelor & Townsend's (1948) lowest-Reynolds-number data. The variation of turbulence Reynolds number with x shown in figure 1 was obtained by solving (2.11*b*) and the turbulence energy equation with f_ϵ taking the form

$$f_\epsilon = 1{\cdot}0 - \frac{0{\cdot}4}{1{\cdot}8}\exp\left[-(\tfrac{1}{6}R_T)^2\right]. \tag{2.12}$$

The corresponding graph of turbulence energy decay is shown in figure 2. In both cases agreement with experimental data is close (as it should be since this is the basis for choosing f_ϵ).

† The individual terms in the two equations should obviously not be paired since those in (2.10) are independent of R_T while those in (2.9) are not.

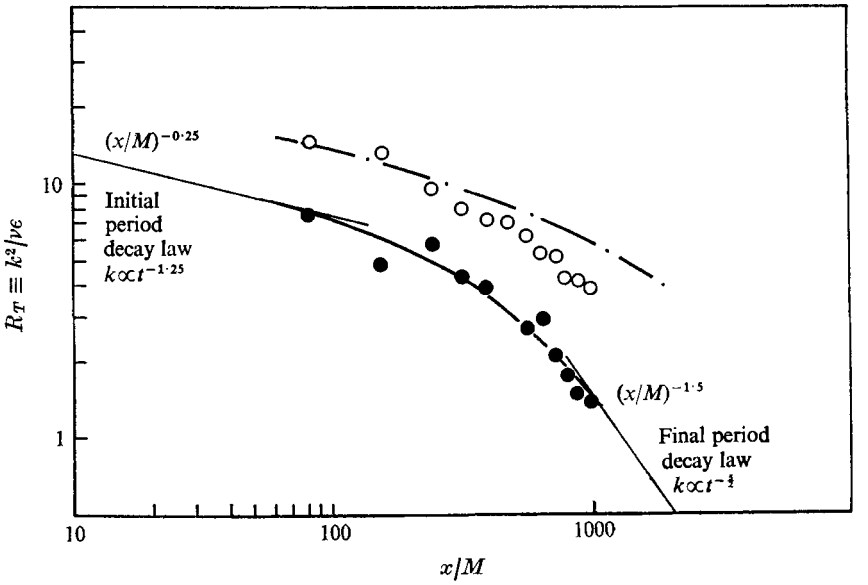

FIGURE 1. Variation of turbulent Reynolds number with distance behind grid: comparison of predictions with Batchelor & Townsend's (1948) experiments. predictions: ——, $Re_M = 650$; —·—, $Re_M = 1360$. Experiment: ●, $Re_M = 650$; ○, $Re_M = 1360$.

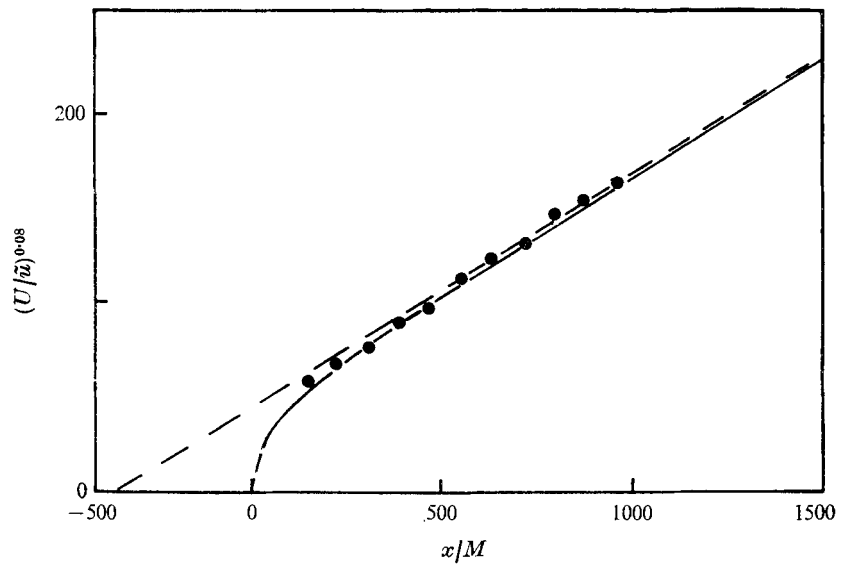

FIGURE 2. Decay of turbulent energy behind grid. ——, predictions; – – –, final-period asymptote; ●, experiment, Batchelor & Townsend (1948), $Re_M = 650$.

The decay term in the dissipative equation requires some further modification before it can be used in the vicinity of a wall. The correlation ϵ takes a non-zero value at the wall while k vanishes; thus the quantity ϵ^2/k tends to infinity, evidently an unacceptable outcome. The difficulty is removed by replacing ϵ^2 by $\epsilon\tilde{\epsilon}$, where the quantity $\tilde{\epsilon}$ is defined as

$$\tilde{\epsilon} \equiv \epsilon - 2\nu\,(\partial k^{\frac{1}{2}}/\partial x_l)^2. \tag{2.13}$$

The appendix shows that $\tilde{\epsilon}$ varies as x_2^2 in the vicinity of the wall. Thus $c_{\epsilon 2}\epsilon\tilde{\epsilon}/k$ tends to a constant value since k also varies as x_2^2.

Now, in (2.9) the viscous diffusion term $\nu\,\partial^2\epsilon/\partial x_k^2$ is the only term apart from (i) and (ii) which does not vanish at the wall. Moreover, the rough estimates of ϵ that can be deduced from experiment (e.g. Laufer 1954) suggest that the dissipation rate varies by only about a factor of two between the wall and the position of its maximum value (at $x_2^+ \simeq 10$); beyond this it quickly displays the x_2^{-1} decay typical of fully turbulent flows near walls. These are hopeful signs because they indicate that the terms in (2.9) that are so far unaccounted for, and for which no measurements are available, exert collectively a fairly secondary influence. The absence of experimental data precludes any serious attempt at modelling these terms individually. It was felt however that the following approach to closing (2.9) at least retained the correct character of the unknown correlations.

(i) The effects of term (iv) in (2.9), comprising the product of mean velocity gradients and dissipative components, were accounted for by letting the coefficient $c_{\epsilon 1}$ in (2.10) become a function of R_T.

(ii) The other mean-field generation process, term (v), was approximated as

$$-2\nu\overline{\frac{u_k\,\partial u_i}{\partial x_l}}\frac{\partial^2 U_i}{\partial x_k\,\partial x_l} = c_{\epsilon 3}\,\nu\frac{k\overline{u_j u_k}}{\epsilon}\left(\frac{\partial^2 U_i}{\partial x_j\,\partial x_l}\right)\left(\frac{\partial^2 U_i}{\partial x_k\,\partial x_l}\right), \tag{2.14}$$

a form which is suggested by Taylor's (1915) vorticity-transport theory.

(iii) Any viscous effects on the diffusion terms were accommodated by allowing c_ϵ to be Reynolds-number dependent.

The precise forms for the above terms were optimized to give best agreement with the turbulence energy profile for values of x_2^+ up to about 40. The technique was to solve simultaneously the kinetic energy and ϵ equations for a uniform-stress wall flow, supplying experimental values for the mean velocity and the Reynolds stresses. As it turned out, these calculations showed that use of (2.14) alone (i.e. with the coefficients of the generative and diffusive terms in (2.10) taking their constant high-Reynolds-number values) could reduce differences between the calculated and measured energy profiles within experimental uncertainty. Accordingly $c_{\epsilon 1}$ and c_ϵ were thereafter taken as constant. The final appearance of the ϵ equation is similar to one for $\tilde{\epsilon}$ developed by Jones & Launder (1972*a*). There is an important difference between the wall boundary conditions however: $\tilde{\epsilon}$ vanishes at the surface whereas ϵ is finite and its gradient zero.

2.3. *A simpler version for thin shear layers*

In thin shear layers only the shear stress significantly affects the mean flow. The possibility thus arises of devising a simpler procedure for calculating the normal

stresses, thus reducing the task of numerical solution. Hanjalić & Launder (1972) adopted such an approach for high-Reynolds-number flows, assuming each of the normal stresses to be proportional to the turbulence energy and thus reducing by two the number of transport equations to be solved.† Precisely the same assumption cannot be made here because $\overline{u_2^2}/k$ falls to zero as the wall is approached. There is, however, an equally simple alternative. The experiments of Laufer (1954), Eckelmann (1970) and others indicate that the correlation coefficient $\overline{u_1u_2}/(\overline{u_1^2}\,\overline{u_2^2})^{\frac{1}{2}}$ takes a constant value of about 0·47 not only over the fully turbulent region but over a considerable portion of the low-Reynolds-number region as well.‡ Moreover, it is known that $\frac{3}{4}(\overline{u_1^2}+\overline{u_2^2})$ is a close approximation to the turbulent kinetic energy, again over the great majority of the flow. From these two facts (and with minor simplification to remove the nonlinear term in $\overline{u_2^2}$) we deduce that

$$\overline{u_2^2} \simeq 4{\cdot}0\overline{u_1u_2}^2/k. \tag{2.15}$$

Now, the shear-stress equation that results from the proposals made in §2.1 takes the following form in a two-dimensional thin shear flow:

$$\frac{D\overline{u_1u_2}}{Dt} = \frac{\partial}{\partial x_2}\left[\left(\nu + 2c_s\frac{\overline{u_2^2}}{\epsilon}k\right)\frac{\partial\overline{u_1u_2}}{\partial x_2} + c_s\frac{\overline{u_1u_2}}{\epsilon}k\frac{\partial\overline{u_2^2}}{\partial x_2}\right]$$
$$-(c_1+f_{s1})\frac{\overline{u_1u_2}}{k}\epsilon - \left(0{\cdot}24\frac{\overline{u_2^2}}{k} + 0{\cdot}18 - 0{\cdot}11\frac{\overline{u_1^2}}{k}\right)k\frac{\partial U_1}{\partial x_2}. \tag{2.16}$$

In (2.16) the first term on the right represents diffusive transport, the second the turbulence-interaction part of the pressure–strain correlation and the low-Reynolds-number part of the dissipation while the third group of terms contains the net effect of shear production and the mean-strain part of the pressure–strain correlation. The diffusion term has only a minor effect on predictions. For this reason we neglect the second part of the diffusion term involving gradients in $\overline{u_2^2}$§; the term is considerably smaller than the primary diffusion term except in the neighbourhood of the maximum shear stress, where in any event stress diffusion will usually be of negligible importance. If $\overline{u_1^2}$ and $\overline{u_2^2}$ are now eliminated as described above from the first and third terms in (2.16) the following equation for the shear stress emerges:

$$\frac{D\overline{u_1u_2}}{Dt} = \frac{\partial}{\partial x_2}\left[\left(\nu + 8{\cdot}0c_s\frac{\overline{u_1u_2}^2}{\epsilon}\right)\frac{\partial\overline{u_1u_2}}{\partial x_2}\right] - (c_1+f_{s1})\frac{\overline{u_1u_2}}{k}\epsilon$$
$$-f_{s2}[1{\cdot}40(\overline{u_1u_2}/k)^2 + 0{\cdot}03]\,k\,\partial U_1/\partial x_2. \tag{2.17}$$

The coefficient f_{s2} in (2.17) should strictly be unity. Initial computations indicated that then the stress-creation term appeared to be somewhat too large in the

† The transport equation for turbulence energy replaced the equations for the three normal stresses.

‡ The correlation coefficient is not constant, of course, near an axis of symmetry for the shear stress then falls to zero while $\overline{u_1^2}$ and $\overline{u_2^2}$ do not. We nevertheless retain the approximation there for the sake of uniformity. Because the shear stress is necessarily small there the numerical solutions are not significantly impaired by this assumption.

§ This neglect simplifies the task of numerical solution.

Coefficient	Value	Equation of first appearance	Basis for choice
c_s	0·11	(2.4)	Values used by LRR in high-Reynolds-number turbulence
c_1	1·50	(2.3)	
c_2	0·40	(2.3)	
c_ϵ	0·15	(2.10)	
$c_{\epsilon 2}$	1·8	(2.10)	Decay of grid turbulence
$c_{\epsilon 1}$	$c_{\epsilon 2} - 3{\cdot}5c_\epsilon$	(2.10)	Consistency with von Kármán constant of 0·42 (see LRR)
$c_{\epsilon 3}$	2·0	(2.14)	Present work: computer optimization

TABLE 1. Coefficients in model of turbulence

Function	Form	First appearance
f_{s1}	$(1+\frac{1}{10}R_T)^{-1}$	(2.7)
f_{s2}	$\exp[-2/(1+\frac{1}{30}R_T)]$	(2.17)
f_ϵ	$1-\frac{0{\cdot}4}{1{\cdot}8}\left[\exp-\left(\frac{R_T}{6}\right)^2\right]$	(2.12)

TABLE 2. Reynolds-number functions in turbulence model

immediate neighbourhood of the wall, owing perhaps to the diminution of the shear-stress correlation coefficient in this region. Accordingly Reynolds-number-dependent forms for f_{s2} were explored, the one finally adopted appearing in table 2.

The corresponding turbulence kinetic energy equation, obtained by contracting the closed form of the Reynolds-stress equation and simplifying the diffusion term as in (2.17), may be written as

$$\frac{Dk}{Dt} = \frac{\partial}{\partial x_2}\left[\left(\nu + 5{\cdot}0c_s\frac{\overline{u_1u_2}^2}{\epsilon}\right)\frac{\partial k}{\partial x_2}\right] - \overline{u_1u_2}\frac{\partial U_1}{\partial x_2} - \epsilon. \tag{2.18}$$

To complete closure, the quantity ϵ is determined from the following transport equation, obtained by eliminating $\overline{u_2^2}$ from the diffusion term in (2.10) and from the right side of (2.14):

$$\frac{D\epsilon}{Dt} = \frac{\partial}{\partial x_2}\left[\left(\nu + c_\epsilon 4{\cdot}0\frac{\overline{u_1u_2}^2}{\epsilon}\right)\frac{\partial \epsilon}{\partial x_2}\right] - c_{\epsilon 1}\frac{\overline{u_1u_2}\epsilon}{k}\frac{\partial U_1}{\partial x_2} - c_{\epsilon 2}f_\epsilon\frac{\epsilon\tilde{\epsilon}}{k} + 4{\cdot}0c_{\epsilon 3}\frac{\overline{u_1u_2}^2}{\epsilon}\left(\frac{\partial^2 U_1}{\partial x_2^2}\right)^2. \tag{2.19}$$

The empirical constants (the c's) and the Reynolds-number functions (the f's) appearing in the above equations are prescribed as in tables 1 and 2.

The computed results presented in §3 have been obtained by solving (2.17)–(2.19) simultaneously with the streamwise momentum and continuity equations. A modified version of the finite-difference procedure of Patankar & Spalding

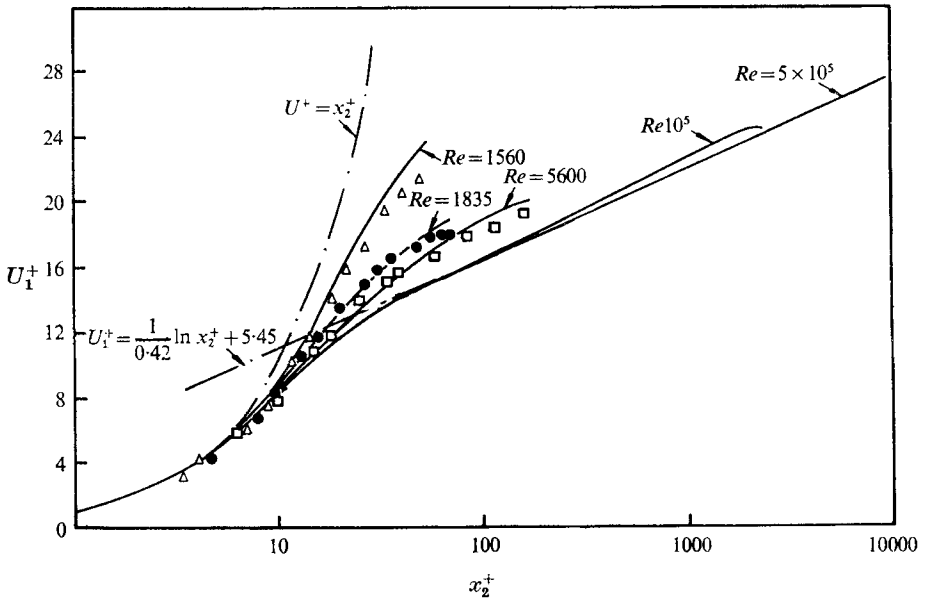

FIGURE 3. Mean velocity profiles in plane channel flow. ——, predictions. Experiment: △, Patel & Head, Re = 1530; ●, Patel & Head, Re = 1835; □, Eckelmann, Re = 5600.

(1970) was developed for this purpose. Ninety cross-stream nodes were used with approximately half of these covering the region between the wall and $x_2^+ \simeq 40$. Forward step sizes were typically 0·2 times the local shear-layer thickness, leading to computing times per run of about 50 s using a CDC 6600 computer.

3. Presentation of results

At high Reynolds numbers the present turbulence model reduces to a form similar to that already proposed and tested by Hanjalić & Launder (1972). Here, therefore, attention is directed mainly to low-Reynolds-number flows, especially under conditions where departure from the usual wall similarity laws occurs. The first class of shear flows examined was fully developed flow in a plane channel of width D. In figure 3 dimensionless mean velocity profiles are shown in the usual semi-logarithmic co-ordinates compared with the experimental data of Patel & Head (1969) and Eckelmann (1970). The numerical predictions correctly display the shift of the velocity profiles progressively above the 'universal' semi-logarithmic law as the Reynolds number is reduced. Quantitative agreement is quite good though it looks as though the predicted 'effective viscosity' is somewhat too low in the core region of the channel since the predicted profiles lie above the measured ones. The predicted profile at Re = 1560 is in fact laminar; repeated attempts to establish a non-trivial solution to the turbulence transport equations (using a variety of initial conditions) all led to the turbulence decaying progressively with distance downstream. Eckelmann measured the turbulent shear-stress profiles at two Reynolds numbers; in figure 4 agreement with his data is seen to be virtually complete. Also shown is the predicted profile for

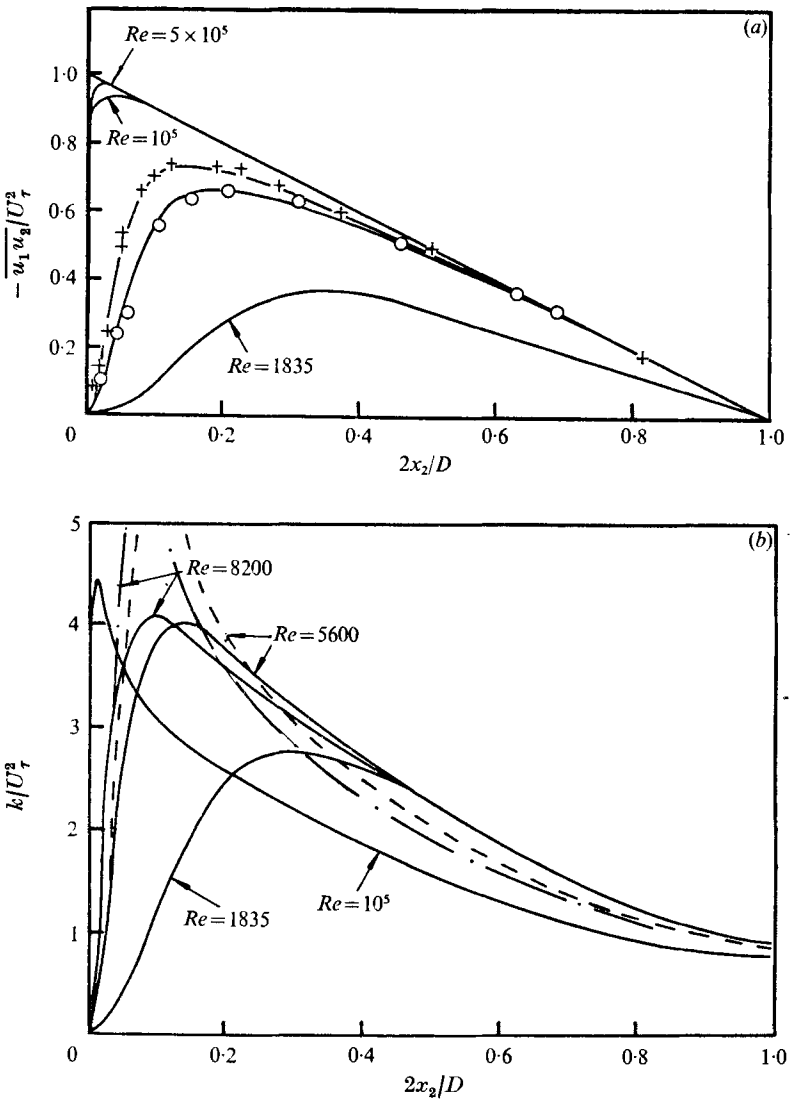

FIGURE 4. (*a*) Shear-stress and (*b*) turbulent energy profiles in a plane channel. ——, predictions. Experiment (Eckelmann 1970): +, —·—, Re = 8200; ○, – – –, Re = 5600.

a bulk-flow Reynolds number of 1835 (which corresponds to one of Patel & Head's experiments shown in figure 3). It is interesting to note that here the peak level of turbulent shear stress is less than 40 % of the wall stress. The corresponding turbulence energy profiles are shown in figure 4 (*b*). Eckelmann did not measure $\overline{u_3^2}$ and the experimental curves were obtained by assuming that $k = \frac{3}{4}(\overline{u_1^2} + \overline{u_2^2})$. The predictions do not match the very steep rise in k close to the wall, predicted peak energy levels being 30 % too low. Elsewhere however agreement is probably satisfactorily close.

The near-wall shear-stress and turbulence kinetic energy profiles are shown in greater detail in figure 5. It may be seen that the predicted turbulence energy

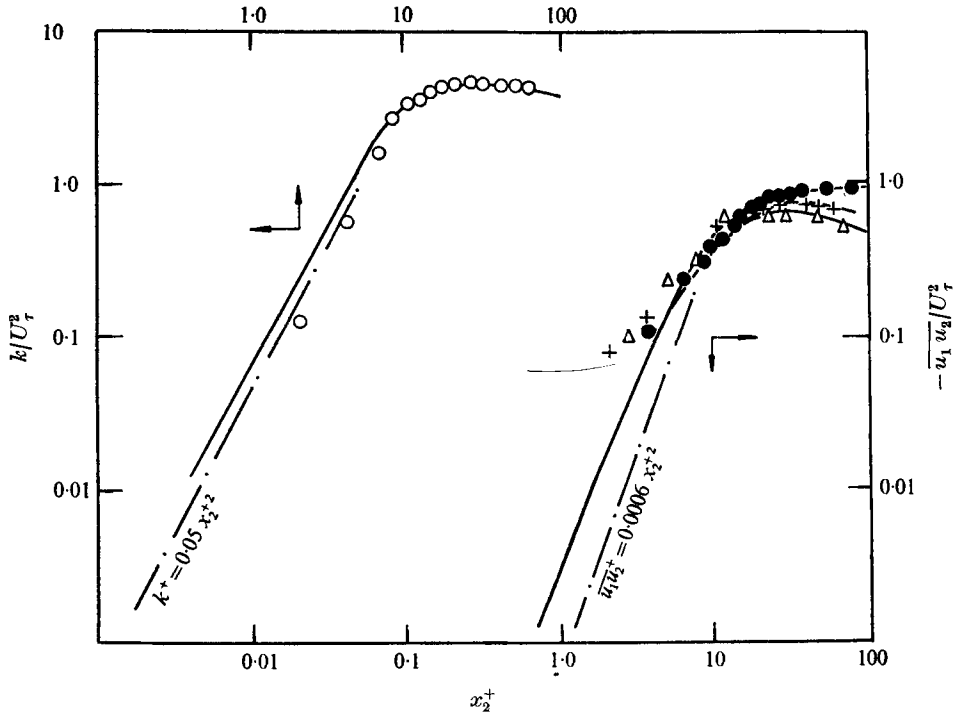

FIGURE 5. Near-wall variation of shear stress and kinetic energy. ——, predictions. Experiment: ○, Laufer (1954), pipe flow, $Re = 5 \times 10^5$; △, Eckelmann (1970), $Re = 5600$; +, Eckelmann (1970), $Re = 8200$; ○, Schubauer (1954), flat plate.

varies as x_2^{+2} for values of x_2^+ up to about 5. The asymptotic value appears to be about 30 % larger than that estimated by Townsend (1956, p. 220) from Laufer's (1954) pipe flow measurements, which suggests that this discrepancy is probably less than possible experimental error. The continuity equation may be used to show that asymptotically $\overline{u_1 u_2}$ varies at least as x_2^{+3}. The predicted variation does display a cubic variation but only for values of x_2^+ below unity. The calculated variation lies well above the formula $\overline{u_1 u_2}^+ = 6 \times 10^{-4} x_2^{+3}$ suggested by Townsend (1956) on the basis of extrapolating Laufer's (1954) pipe flow data. By way of contrast Eckelmann's data scatter above the predicted line for $x_2^+ < 5$, so it is probably fair to say that the present predictions lie within experimental uncertainty. The matter is, in any event, rather academic since over the region in question molecular stress far outweighs the turbulent stress.

We turn now to the accelerating sink-flow boundary layers studied by Jones & Launder (1972*b*). Figure 6 compares the predicted profiles for this self-preserving flow with the velocity profile measured at the final station. As in the case of low-Reynolds-number channel flow, the mean velocity profile lies well above Patel's law-of-the-wall line. The current model achieves satisfactory agreement with measurement except within the range $20 < x_2^+ < 90$. The predicted solution lacks the knuckle that is present in the measurements or, in other words, the computed profile exhibits too gradual a changeover from a viscous behaviour near the wall

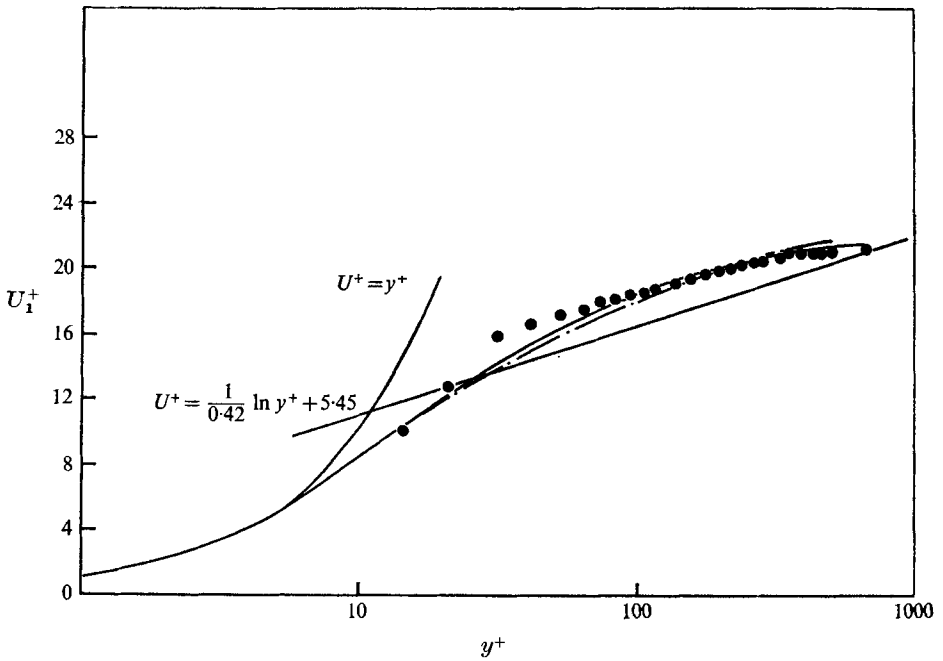

FIGURE 6. Sink-flow turbulent boundary layer; $(\nu/U_{1G}^2)\, dU_{1G}/dx = 1{\cdot}5 \times 10^6$. ——, present predictions; ●, experiment, Jones & Launder (1972*b*); – – –, predictions, Jones (1971).

to fully turbulent behaviour in the outer region. Also shown in figure 6 is Jones' (1971) prediction of the same set of experimental data. The model used for his computations was similar in some respects to the present one (transport equations being solved for k and ϵ) except that the turbulent-viscosity hypothesis was used in place of a shear-stress equation (see Jones & Launder 1972*a*). The velocity profile generated by this model also predicts the departure of the profile above the semi-logarithmic line but generally the profile shape is less accurately predicted than with the present model.

The final comparisons are drawn with another accelerating flow experiment (Launder 1964) only unlike the previous example, the flow is now by no means self-preserving. A flat-plate boundary layer is subjected to a severe acceleration† which increases the free-stream velocity by 2·6 : 1; thereafter the flow develops in essentially uniform pressure. Figure 7, which shows the variation of the shape factor through the test section, provides a summary of the changes in the boundary-layer structure that take place. The initial fall in the shape factor H is typical of the behaviour of accelerated turbulent boundary layers; the sharp rise in H is associated with the reversion of the boundary layer to a viscous one; and the equally sharp fall in shape factor is due to a reversion of the flow to turbulent some distance downstream from the acceleration. In this case the predicted flow behaviour is fairly sensitive to the initial profiles of k and ϵ, neither of which were measured in the experiment. To convey an impression of the influence of such

† The maximum level of $\nu/U_{1G}^2(dU_{1G}/dx)$ (U_{1G} being the free-stream velocity) is approximately 3×10^{-5} compared with $1{\cdot}5 \times 10^{-6}$ in the sink-flow experiment shown in figure 6.

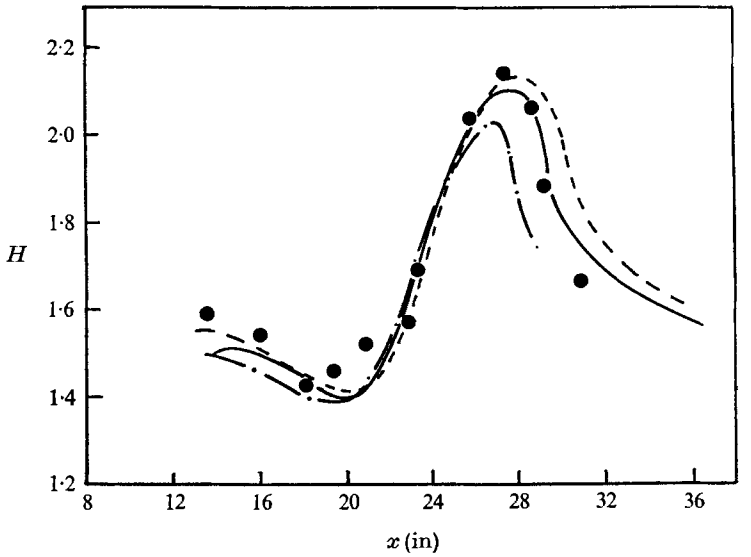

FIGURE 7. Non-equilibrium, strongly accelerating boundary layer: comparison of predictions (curves) with measurements of Launder (1964; points) for different initial conditions.

uncertainties three sets of predictions are shown in figure 7, providing a moderate range of plausible initial values. The acrobatic behaviour of the shape factor is quite well mirrored by these predictions. From these comparisons it is clear that the numerical computations do indeed produce broadly the same behaviour as displayed by the experiment. More than that cannot yet be claimed for if the precise initial conditions were known it is possible that these would lead to worse agreement than is shown in figure 7.

4. Concluding remarks

The present work has attempted to develop a second-order closure scheme for the region of low-Reynolds-number turbulence adjacent to a wall, the starting point being the high-Reynolds-number form of LRR. The rigour achieved is not entirely even: the closure of the dissipation equation has had to rely on more directly empirical inputs than that for the stress equations. However, the same difficulty exists even at high Reynolds numbers. An encouraging level of agreement with experiment has been obtained in a number of flows where the region of low-Reynolds-number turbulence is especially influential. In particular the model predicts the sink-flow boundary layer more accurately than the similar but simpler model of Jones & Launder (1972*a*), presumably because the latter, through the use of the turbulent-viscosity concept, neglects convective transport of shear stress.

The present closure makes two further improvements on that earlier model. The first is the use of an equation for ϵ rather than $\tilde{\epsilon}$. The second and fundamentally more important one is connected with the use of (2.15) to eliminate $\overline{u_2^2}$. The model of Jones & Launder, in common with virtually every other proposal

for treating the near-wall regions, implicitly assumes proportionality of $\overline{u_2^2}$ and k. As remarked in § 2, however, the ratio $\overline{u_2^2}/k$ in fact diminishes progressively as the wall is approached. This inherent weakness passes unnoticed because of the necessity (as in the present work) of allowing a Reynolds-number dependence to appear in some terms; the variation of $\overline{u_2^2}/k$ simply gets absorbed in the empirical Reynolds-number function or functions. However, a legacy of this arrangement is that direct viscous influences on turbulence are deemed to extend to Reynolds numbers many times higher than in free flows. By contrast, in the present model, the function f_ϵ (devised by reference to the final period of decay of grid turbulence) acts over about the same range of R_T as does f_s, the Reynolds-number-dependent function in the stress equation.

Finally, a cautionary note needs to be sounded. The current proposals relate only to regions of low-Reynolds-number turbulence adjacent to a wall. It would not be appropriate to apply the present closure to low-Reynolds-number phenomena in free shear flows.

The research has been supported by the Science Research Council through grant B/RG/1863. One of us (K.H.) acknowledges with thanks the award of an S.R.C. Senior Visiting Fellowship during a period of study leave from the Mašinski Fakultet, Sarajevo.

Appendix

In the immediate vicinity of a wall the fluctuating velocity components may be expressed as

$$\left.\begin{aligned} u_1 &= a_1 x_2 + a_2 x_2^2 + \ldots, \\ u_2 &= \quad\; b_2 x_2^2 + \ldots, \\ u_3 &= c_1 x_2 + c_2 x_2^2 + \ldots, \end{aligned}\right\} \tag{A 1}$$

where the a's, b's and c's are functions of x_1, x_3 and t with average value zero. From (A 1) it is readily deduced that the turbulence kinetic energy near a wall varies according to

$$k = \tfrac{1}{2}(\overline{a_1^2} + \overline{c_1^2})\, x_2^2 + (\overline{a_1 a_2} + \overline{c_1 c_2}) x_2^3 + O[x_2^4].$$

For compactness replace $\frac{1}{2}(\overline{a_1^2} + \overline{c_1^2})$ by a^2 and $(\overline{a_1 a_2} + \overline{c_1 c_2})$ by b. Thus we infer

$$k^{\frac{1}{2}} = a x_2 (1 + \tfrac{1}{2} b a^{-2} x_2 + \ldots O[x_2^2]),$$

from which it is easily demonstrated that

$$(\partial k^{\frac{1}{2}}/\partial x_2)^2 = a^2 + 2 b x_2 + O[x_2^2]. \tag{A 2}$$

Turning now to the dissipative correlation, use of (A 1) retaining first- and second-order terms gives

$$\epsilon/\nu \equiv \overline{(\partial u_i/\partial x_k)^2} = (\overline{a_1^2} + \overline{c_1^2}) + 4(\overline{a_1 a_2} + \overline{c_1 c_2})\, x_2 + O[x_2^2],$$

or

$$\epsilon = 2\nu a^2 + 4\nu b x_2 + O[x_2^2]. \tag{A 3}$$

We thus conclude from (A 2) and (A 3) that the 'isotropic' part of the dissipation rate, $\tilde{\epsilon} \equiv \epsilon - 2\nu(\partial k^{\frac{1}{2}}/\partial x_2)^2$, varies as x_2^2 in the neighbourhood of the wall since the leading terms in these two equations cancel.

REFERENCES

BATCHELOR, G. K. & TOWNSEND, A. A. 1948 Decay of isotropic turbulence in the final period. *Proc. Roy. Soc.* A **194**, 538.

BECKWITH, I. E. & BUSHNELL, D. 1968 Detailed description and results of a method for computing mean and fluctuating quantities in turbulent boundary layers. *N.A.S.A. Tech. Note*, D-4815.

BRADSHAW, P., FERRISS, D. H. & ATWELL, N. P. 1967 Calculation of boundary-layer development using the turbulent energy equation. *J. Fluid Mech.* **28**, 593.

COMTE-BELLOT, G. & CORRSIN, S. 1966 The use of a contraction to improve the isotropy of grid-generated turbulence. *J. Fluid Mech.* **25**, 657.

DALY, B. J. & HARLOW, F. H. 1970 Transport equations in turbulence. *Phys. Fluids*, **13**, 2634.

ECKELMANN, H. 1970 Experimentelle Untersuchungen in einer turbulenten Kanalströmung mit starken viskosen Wandschichten. *Mitt. Max-Planck Inst. f. Strömungsforschung, Göttingen*, no. 48.

GLUSHKO, G. 1965 Turbulent boundary layer on a flat plate in an incompressible fluid. *Izv. Acad. Nauk SSSR Mekh.* no. 4, p. 13.

HANJALIĆ, K. & LAUNDER, B. E. 1972 A Reynolds stress model of turbulence and its application to thin shear layers. *J. Fluid Mech.* **52**, 609.

HINZE, J. O. 1959 *Turbulence.* McGraw-Hill.

JONES, W. P. 1971 Laminarisation in strongly accelerated boundary layers. Ph.D. thesis, University of London.

JONES, W. P. & LAUNDER, B. E. 1972*a* The predictions of laminarisation with a two-equation model of turbulence. *Int. J. Heat Mass Transfer*, **15**, 301.

JONES, W. P. & LAUNDER, B. E. 1972*b* Some properties of sink-flow turbulent boundary layers. *J. Fluid Mech.* **56**, 337.

JONES, W. P. & LAUNDER, B. E. 1973 The calculation of low-Reynolds-number phenomena with a two-equation model of turbulence. *Int. J. Heat Mass Transfer*, **16**, 1119.

LAUFER, J. 1954 The structure of turbulence in fully developed pipe flow. *N.A.C.A. Rep.* no. 1033.

LAUNDER, B. E. 1964 Laminarisation of the turbulent boundary layer by acceleration. *M.I.T. Gas Turbine Lab. Rep.* no. 77.

LAUNDER, B. E., REECE, G. J. & RODI, W. 1975 Progress in the development of a Reynolds-stress turbulence closure. *J. Fluid Mech.* **68**, 537.

LUMLEY, J. L. 1972 A model for computation of stratified turbulent flow. *Proc. Int. Symp. on Stratified Flow, Novisibirsk.*

LUMLEY, J. L. & KHAJEH NOURI, B. 1973 Modelling homogeneous deformation of turbulence. *Pennsylvania State University Rep.*

PATANKAR, S. V. & SPALDING, D. B. 1970 *Heat and Mass Transfer in Boundary Layers.* London: Intertext.

PATEL, V. C. & HEAD, M. R. 1969 Some observations of skin friction and velocity profiles in fully developed pipe and channel flows. *J. Fluid Mech.* **38**, 181.

PRANDTL, L. 1945 Über eine neues Formelsystem für die ausgebildete Turbulenz. *Nachr. Akad. Wiss., Göttingen, Mathphys*, p. 16.

ROTTA, J. C. 1951 Statistische Theorie nichthomogener Turbulenz. *Z. Phys.* **129**, 547.

REYNOLDS, W. C. 1970 Computation of turbulent flows-state-of-the-art. *Stanford University, Mech. Engng Dept. Rep.* MD-27.

SCHUBAUER, G. B. 1954 Turbulent processes as observed in boundary layer and pipes. *J. Appl. Phys.* **25**, 188.

TAYLOR, G. I. 1915 *Phil. Trans.* A **215**, 1.

TENNEKES, H. & LUMLEY, J. L. 1972 *A First Course in Turbulence.* M.I.T. Press.

TOWNSEND, A. A. 1956 *The Structure of Turbulent Shear Flow.* Cambridge University Press.

VAN DRIST, E. R. 1956 On turbulent flow near a wall. *J Aero. Sci.* **23**, 1007.

WOLFSHTEIN, M. 1969 The velocity and temperature distribution in one-dimensional flow with turbulence augmentation and pressure gradient. *Int. J. Heat Mass Transfer*, **12**, 301.